Electronic Supplementary Material (ESI) for Journal of Materials Chemistry C.

Electronic Supplementary Information

Phosphorescent Pt (II) Acetylacetonate Complexes Bearing 9-(pyrimidin-2-yl)-9H-carbazole Ligand: Syntheses, Photophysical Properties and OLEDs Applications

Haibo Yao,[†a,b] Lequn Yuan,[†a] Ling Pei,[b] Yunjun Shen,[a] Yuzhen Zhang,*[a] Liang Zhou,*[c] Hedong Bian,*[a]

[a] Key Laboratory of Chemistry and Engineering of Forest Products, State Ethnic Affairs Commission, Guangxi Key Laboratory of Chemistry and Engineering of Forest Products, Guangxi Collaborative Innovation Center for Chemistry and Engineering of Forest Products, School of Chemistry and Chemical Engineering, Guangxi Minzu University, Nanning 530006, Guangxi, China.

E-Mail: zhangyuzhen@gxmzu.edu.cn. gxunchem@163.com

[b] Engineering Research Center for Industrial Wastewater Treatment and Reuse of Shandong Province, School of Chemical Engineering and Safety, Binzhou University, Binzhou 256603, Shandong, China.

[c] State Key Laboratory of Rare Earth Resource Utilization, Changchun Institute of Applied Chemistry, Chinese Academy of Sciences, Changchun 130022, P. R. China.

E-mail: zhoul@ciac.ac.cn

Table of Contents

General Information

Chemicals

All commercially chemicals are directly purchased without further purification. All commercial reagents were purchased from standard suppliers and were used without further purification.

Characterization

Thin-layer chromatography (TLC) was carried out using silica gel 60, F254 with a thickness of 0.25 mm. Column chromatography was performed on silica gel 60 (200-300 mesh).

NMR spectra were recorded on a Bruker AVANCE III 400 spectrometers (^{1}H NMR 400 MHz, ^{13}C NMR 100 MHz) at 25 °C. Data are reported as follows: Chemical shift in ppm, multiplicity (s = singlet, d = doublet, t = triplet, q = quartet, m = multiplet, dd = doublet of doublets, etc.), coupling constant *J* in Hz, integration, and (where applicable) interpretation.

High-resolution MS data were recorded using ThermoFisher Scientific (USA) equipped with an electrospray ionization source (ESI). Accurate mass determination was corrected by calibration using sodium trifluoroacetate clusters as a reference.

Single-crystal X-ray diffraction studies were performed on Bruker D8 Venture using Mo radiation. Olex2 was used in the determination of these structures.

UV−vis absorption measurements were carried out on an Agilent's Cary 100 UV−vis spectrophotometer. Emission spectrum, phosphorescence lifetime and quantum yield were measured directly using Edinburgh Instruments model FLS1000.

Cyclic voltammetry measurements were performed using a CHI 760E electrochemical workstation equipped with a glassy carbon working electrode (d = 2 mm), platinum wire counter electrode, Pt counter electrode, and Ag^{+}/Ag reference electrode. ACS reagent grade solvents were used for the measurements, and the solutions were bubbled with nitrogen for 15 min prior to the test.

The theoretical calculations of the Pt (II) were performed using Gaussian 09 program.[1] The geometries of the ground state S_0 were optimized with the density functional

theory (DFT) method with the B3LYP function. The 6-31G (d, p) basis set was used for the C, H, N, and O atoms and LanL2DZ basis set was employed for the Pt atoms. Considering the solvent effect, the DCM was taken as the solvent into the polarizable continuum model (PCM) when the optimizations were conducted. The energies of the singlet and triplet excited states were obtained from the time-dependent density functional theory (TD-DFT) calculations. All molecular structures and orbital compositions were analyzed by Multiwfn [2] and visualized by VMD. [3]

All organic materials used in this study were obtained commercially and used as received without further purification except for compounds **2a** and **4a**, which were synthesized and purified experimentally. Indium tin oxide (ITO) coated glass (10 Ω sq^{-1}) was used as the anode substrate. Before device preparation, the ITO glass substrate needs to be carefully cleaned with detergent and ultrasound, and finally placed in an oven for drying. All organic layers were deposited in the organic vacuum chamber at a rate of 0.01 nm s^{-1} under vacuum pressure below 3×10^{-6} Pa. LiF and Al were deposited in the metal vacuum chamber at the rates of 0.01 nm s^{-1} and 0.5 nm s^{-1}, respectively, under vacuum pressure below 3×10^{-6} Pa. Current density-voltage-luminance (*J-V-L*) characteristics, EQE, $CIE_{x,y}$, and EL spectra were measured using M6100 OLED IVL test system.

Experimental Section

The primary ligand of 3,6-Di-tert-butyl-9-(pyrimidin-2-yl)-9H-carbazole ($TBPCH_2$) was prepared by following the reported procedure.[4]

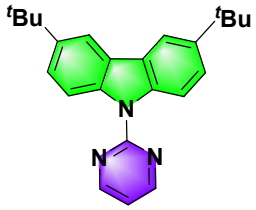

General procedure for synthesizing ligand $TBPCH_2$

2-bromopyrimidine (1.02 g, 6.44 mmol), 3,6-Di-tert-butyl-9H-carbazole (1.50 g, 5.37 mmol), CuCl (4.95mg, 0.06 mmol), *t*-BuOLi (645 mg, 8.06mmol) were added in to a 200 mL one-necked Schlenk flask equipped with a magnetic stirring bar and extracted air for 10 min under the vacuum condition. Then 1-methy-1*H*-imidazole (0.86 mL, 10.7 mmol) and anhydrous and anaerobic toluene solution 50 mL were added into the flask under nitrogen atmosphere. The resulting mixture was bubbled with nitrogen for 10

min and then heated at 130 °C under nitrogen condition for 36 hours. After cooling down to room temperature, the solvent was removed. The residue was extracted with EtOAc. The organic fraction was collected and dried with $MgSO_4$. After the filtration, the solvent was removed and the crude product was purified by silica column chromatography with eluent of EtOAc and *n*-hexane (1:25) to obtain a white powder 1.56g, 81% yield.

$TBPCH_2$: ^{1}H NMR (400 MHz, $CDCl_3$, δ, ppm): 8.81 – 8.76 (m, 4H), 8.07 (d, *J* = 1.8Hz, 2H), 7.57 – 7.54 (m, 2H), 7.06 (t, *J* = 4.5Hz, 1H), 1.48 (s, 18H). ^{13}C NMR (100 MHz, $CDCl_3$, δ, ppm): 159.22, 157.80, 145.26, 137.51, 125.88, 124.21, 115.92, 115.52, 34.75, 31.87. Elemental analysis: Calc. for $C_{24}H_{27}N_3$: C, 80.63%; H, 7.61%; N, 11.75%. Found: C, 80.35%; H, 7.48%; N, 11.82%.

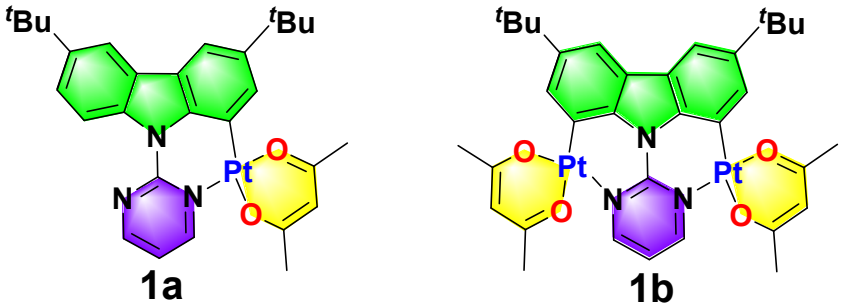

General procedure for synthesizing complexes 1a and 1b.

3,6-Di-tert-butyl-9-(pyrimidin-2-yl)-9H-carbazole ($TBPCH_2$) (536 mg, 1.50 mmol) was added into a 200 mL one-necked Schlenk flask equipped with a magnetic stirring bar and extracted air for 10 min under the vacuum condition. After filling with nitrogen, a solution of K_2PtCl_4 (1.25 g, 3.01 mmol) in minor water and 70 mL glacial acetic acid were injected into the flask. The resulting mixture was bubbled with nitrogen for 10 min and then refluxed under nitrogen condition for 24 hours. The mixture was cooled to room temperature and then kept into ice bath for 2 hours, the precipitate was filtered by filtration and washed with water for 3 times and dried with vacuum to generate dichloro-bridged intermediate 1.05 g (1.29 mmol, yield: 85%, calculated based on the molecular weight of binuclear polymer $[Pt_2(TBPC)(\mu\text{-}Cl)_2]_n$). These Intermediate products was not purified anymore and used for the next step directly. The dichloro-bridged intermediate (150 mg, 0.180 mmol), acetylacetone (acacH) (0.05 mL, 0.49 mmol), aqueous K_2CO_3 solution (4.0 mL, 0.98 mmol) and acetone 50 mL were transferred into a Schlenk flask and stirred at reflux condition under nitrogen atmosphere for 18 hrs. After cooling down to room temperature, the solvent was

removed. The residue was extracted with DCM. The organic fraction was collected and dried with $MgSO_4$. After the filtration, the solvent was removed and the crude product was purified by silica column chromatography with eluent of CH_2Cl_2 and *n*-hexane. Two complexes was isolated from the crude product: mononuclear product **1a** with yellow colour Pt(TBPCH)(acac) CH_2Cl_2/hexane (1:3), 52 mg, 44% yield; binuclear products **1b** with orange colour Pt_2(TBPC)(acac)$_2$ CH_2Cl_2/hexane (1:1), 20 mg, 11% yield.

1a ^{1}H NMR (400 MHz, $CDCl_3$, δ, ppm): δ 9.62 (dd, *J* = 6.2, 2.3 Hz, 1H), 8.76 (dd, *J* = 4.3, 2.3 Hz, 1H), 8.72 (d, *J* = 8.8 Hz, 1H), 7.99 (d, *J* = 2.1 Hz, 1H), 7.81 (d, *J* = 1.9 Hz, 1H), 7.68 (d, *J* = 1.9 Hz, 1H), 7.49 (dd, *J* = 8.8, 2.1 Hz, 1H), 6.87 (dd, *J* = 6.2, 4.3 Hz, 1H), 5.50 (s, 1H), 2.04 (s, 3H), 1.99 (s, 3H), 1.47 (d, *J* = 8.6 Hz, 18H). ^{13}C NMR (100 MHz, $CDCl_3$, δ, ppm): 186.21, 184.69, 158.90, 156.73, 150.71, 146.60, 145.18, 137.94, 136.80, 128.94, 127.35, 123.36, 121.87, 118.80, 116.04, 113.28, 112.23, 102.03, 101.66, 35.15, 34.78, 31.96, 31.78, 28.33, 26.92. HRMS (ESI): *m/z* Calcd. for $C_{29}H_{33}N_3O_2PtH$, $[M+H]^+$: 651.2293. Found: 651. 2294. Elemental analysis: Calc. for $C_{29}H_{33}N_3O_2Pt{\cdot}0.5H_2O$: C, 52.80%; H, 5.20%; N, 6.37% found: C, 52.81%; H, 4.88%; N, 6.40%.

1b ^{1}H NMR (400 MHz, $CDCl_3$, δ, ppm): 9.48 (d, *J* = 5.9 Hz, 2H), 7.59 (dd, *J* = 12.0, 1.9 Hz, 4H), 6.61 (t, 1H), 5.48 (s, 2H), 2.03 (s, 6H), 1.96 (s, 6H), 1.45 (s, 18H). ^{13}C NMR (100 MHz, $CDCl_3$, δ, ppm): 186.37, 184.70, 159.50, 147.33, 143.24, 136.42, 126.74, 125.82, 113.16, 111.02, 103.60, 101.98, 35.15, 31.81, 28.23, 26.78. HRMS (ESI): *m/z* Calcd. for $C_{34}H_{39}N_3O_4Pt_2H$, $[M+H]^+$: 943.2288. Found: 943.2298. Elemental analysis: Calc. for $C_{34}H_{39}N_3O_4Pt_2{\cdot}CH_2Cl_2$: C, 40.86%; H, 4.02%; N, 4.08%. Found: C, 41.05%; H, 4.18%; N, 4.12%.

Synthetic procedure for complex 2a. Following the general procedure of preparing complex **1a**. The ancillary ligand of dipivaloylmethane (dpmn) (0.11 mL, 0.50 mmol) was used to prepare complex **2a,** 81 mg, 61% yield.

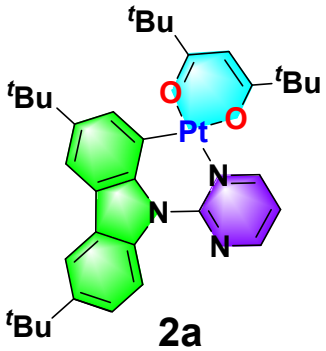

2a

2a ^{1}H NMR (400 MHz, $CDCl_3$, δ, ppm): δ 9.63 (dd, *J* = 6.2, 2.3 Hz, 1H), 8.77 (dd, *J* = 4.3, 2.3 Hz, 1H), 8.71 (d, *J* = 8.8 Hz, 1H), 7.99 (d, *J* = 2.0 Hz, 1H), 7.85 (d, *J* = 1.9 Hz, 1H), 7.68 (d, *J* = 1.9 Hz, 1H), 7.48 (dd, *J* = 8.8, 2.1 Hz, 1H), 6.87 (dd, *J* = 6.2, 4.3 Hz, 1H), 5.85 (s, 1H), 1.47 (d, *J* = 9.9 Hz, 18H), 1.31 (s, 9H), 1.24 (s, 9H). ^{13}C NMR (100 MHz, $CDCl_3$, δ, ppm): 195.59, 194.51, 158.88, 156.79, 150.95, 146.58, 145.37, 138.21, 136.76, 129.07, 128.15, 123.29, 121.79, 118.74, 116.03, 113.06, 111.98, 103.09, 92.98, 41.48, 41.28, 35.05, 34.77, 32.11, 31.79, 28.85, 28.37. HRMS (ESI): *m/z* Calcd. for $C_{35}H_{45}N_3O_2PtH$, $[M+H]^+$: 735.3232. Found: 735.3232. Elemental analysis: Calc. for $C_{35}H_{45}N_3O_2Pt{\cdot}2H_2O$: C, 54.53%; H, 6.41%; N, 5.45%. Found: C, 54.85%; H, 6.58%; N, 5.52%.

Synthetic procedure for complex 3a. Following the general procedure. The ancillary ligand of dibenzoylmethane (dbmn) (101 mg, 0.450 mmol) was used to prepare complex **3a**, 77 mg, 55% yield.

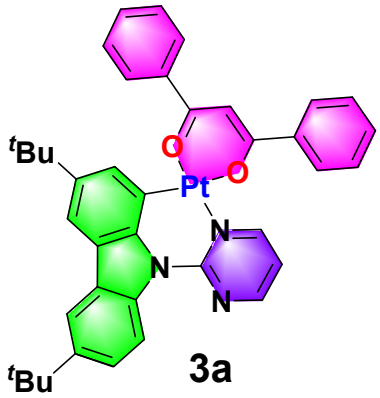

3a

3a ^{1}H NMR (400 MHz, $CDCl_3$, δ, ppm): 9.76 (dd, *J* = 6.2, 2.3 Hz, 1H), 8.79 – 8.78 (q, 1H), 8.72 (d, *J* = 8.8 Hz, 1H), 8.12 – 8.11 (m, 2H), 8.01 – 7.96 (m, 4H), 7.72 (d, *J* = 1.8 Hz, 1H), 7.60 – 7.54 (m, 2H), 7.51 – 7.43 (m, 5H), 6.94 – 6.92 (q, 1H), 6.80 (s, 9H), 1.53 (s, 9H), 1.47 (s, 9H). ^{13}C NMR (100 MHz, $CDCl_3$, δ, ppm): 179.32, 178.78, 158.01, 155.87, 149.92, 145.64, 144.47, 138.80, 137.87, 137.12, 135.77, 130.09, 129.97, 127.98, 127.65, 127.42, 126.75, 126.38, 125.99, 122.38, 120.96, 117.80, 115.02, 112.28, 111.30, 101.05, 95.80, 34.11, 33.74, 31.04, 30.74. HRMS (ESI): *m/z* Calcd. for $C_{39}H_{37}N_3O_2PtH$, $[M+H]^+$: 775.2606. Found: 775.2601. Elemental analysis: Calc. for $C_{39}H_{37}N_3O_2Pt{\cdot}H_2O$: C, 59.08%; H, 4.96%; N, 5.30%. Found: C, 59.33%; H, 4.58%; N, 5.28%.

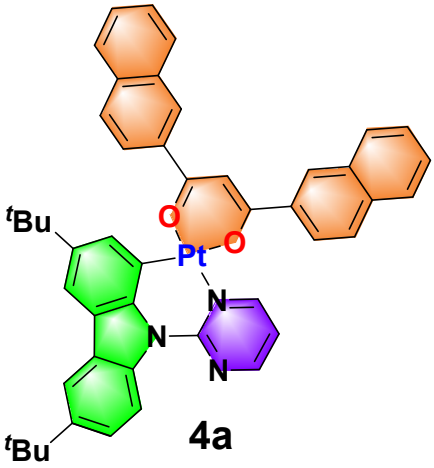

4a

Synthetic procedure for complex 4a. Following the general procedure. The ancillary ligand of di(2-naphthoyl) methane (dnmn) (146 mg, 0.450 mmol) was used to prepare complex **4a**, 45 mg, 29% yield.

4a ^{1}H NMR (400 MHz, $CDCl_3$, δ, ppm): 9.82 (dd, *J* = 6.2, 2.3 Hz, 1H), 8.72 – 8.71 (q, 1H), 8.70 – 8.67 (d, *J* = 8.8 Hz, 1H), 8.61 (s, 1H), 8.47 (s, 1H), 8.16 (dd, *J* = 8.7, 1.8 Hz, 1H), 8.06 – 7.96 (m, 5H), 7.87 – 7.85 (m, 4H), 7.71 (d, *J* = 1.9 Hz, 1H), 7.61 – 7.47 (m, 5H), 7.03 (s, 1H), 6.87 (dd, *J* = 6.2, 4.3 Hz, 1H), 1.57 (s, 9H), 1.48 (s, 9H). ^{13}C NMR (100 MHz, $CDCl_3$, δ, ppm): 180.12, 179.63, 159.18, 156.91, 151.05, 146.74, 145.55, 138.32, 137.25, 136.94, 136.53, 134.71, 133.14, 133.07, 129.22, 129.16, 129.12, 128.66, 128.48, 128.21, 127.97, 127.72, 127.63, 127.55, 127.46, 126.96, 126.82, 126.72, 124.56, 124.06, 123.53, 122.12, 119.01, 116.16, 113.39, 112.37, 102.49, 97.69, 35.34, 34.92, 32.38, 31.93. HRMS (ESI): *m/z* Calcd. for $C_{47}H_{41}N_3O_2PtH$, $[M+H]^+$: 875.2919. Found: 875.2918. Elemental analysis: Calc. for $C_{47}H_{41}N_3O_2Pt{\cdot}CH_2Cl_2$: C, 60.06%; H, 4.52%; N, 4.38%. Found: C, 59.71%; H, 4.20%; N, 4.48%.

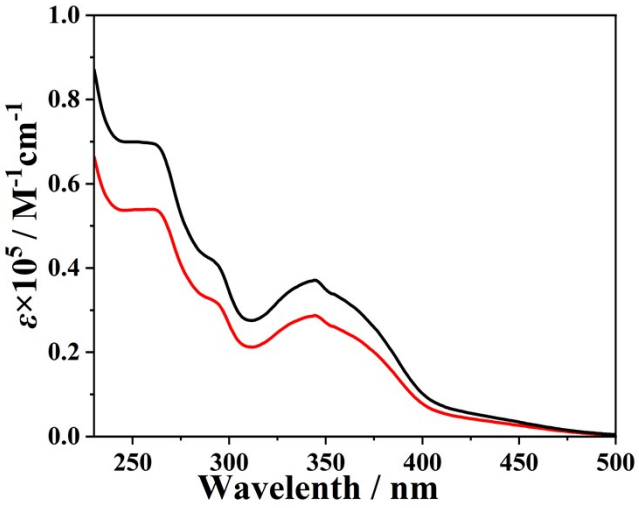

Figure S1. UV–Vis absorption spectra of **4a-y** (black) and **4a-r** (red) in CH_2Cl_2 at r.t.

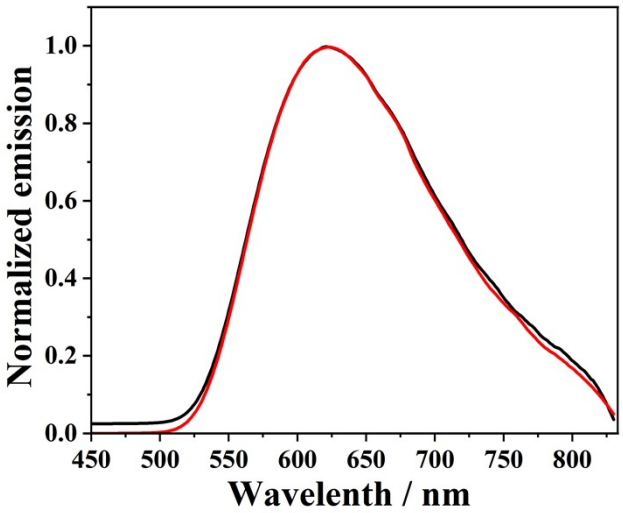

Figure S2. Normalized emission spectra of **4a-y** (black) and **4a-r** (red) in deoxygenated CH_2Cl_2 at r.t.

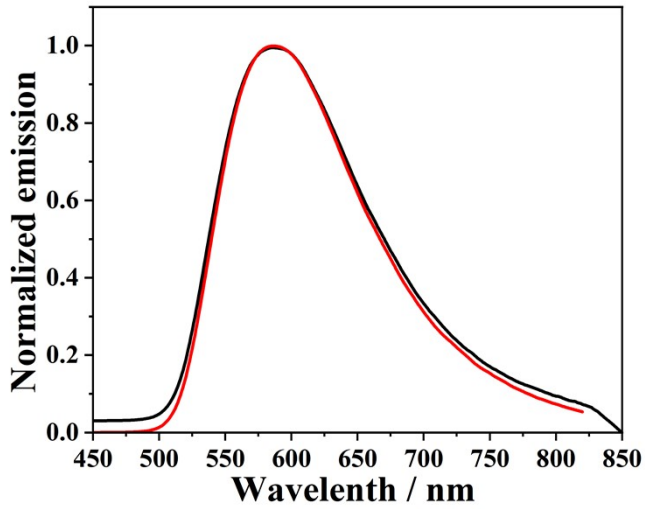

Figure S3. Normalized emission spectra of **4a-y** (black) and **4a-r** (red) in 2 wt% PMMA film.

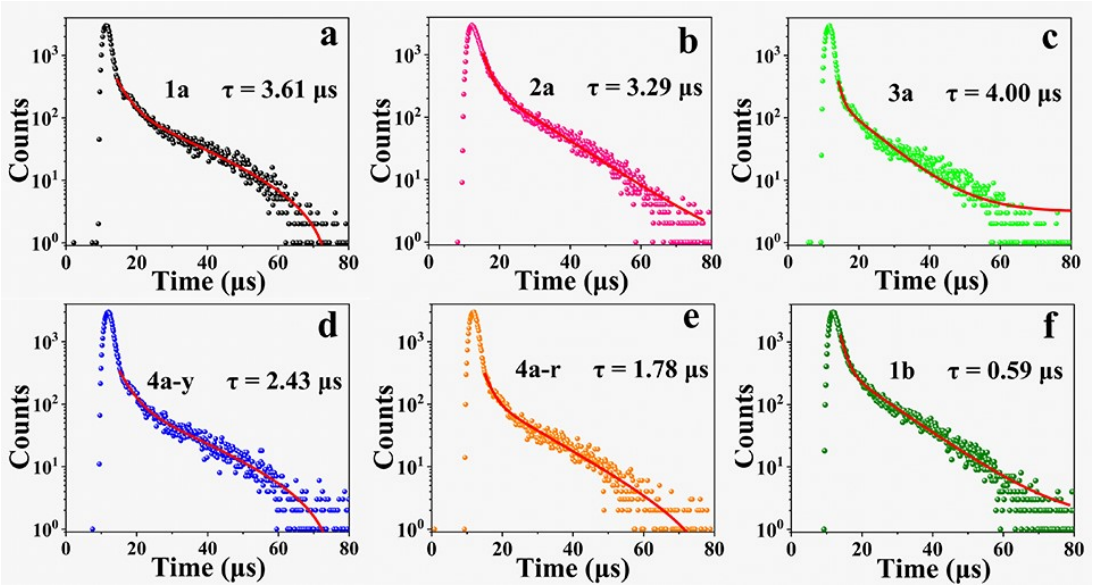

Figure S4. PL decay curves of all the complexes in solid state at r.t

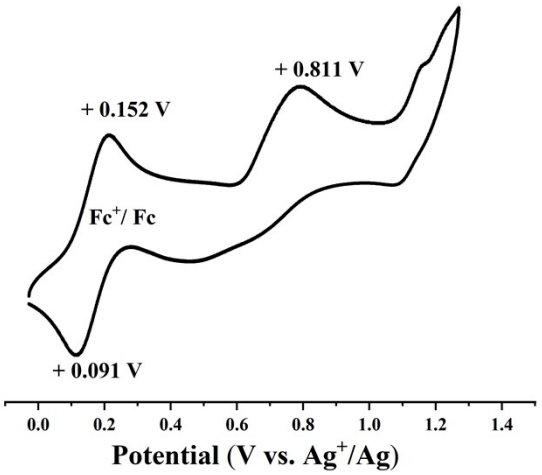

Figure S5. The cyclic voltammograms spectra of **1a** with Fc+/ Fc.

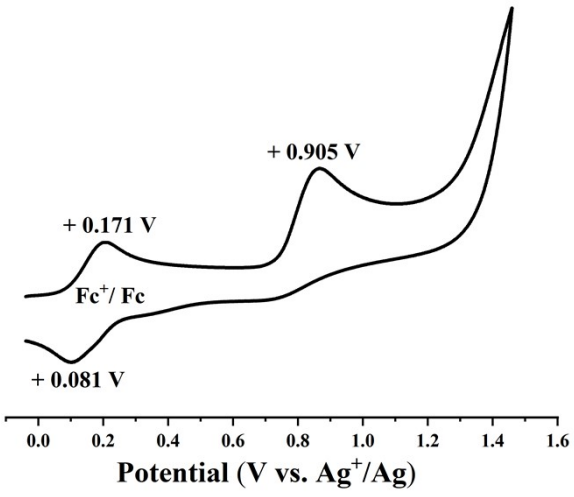

Figure S6. The cyclic voltammograms spectra of **2a** with Fc+/ Fc.

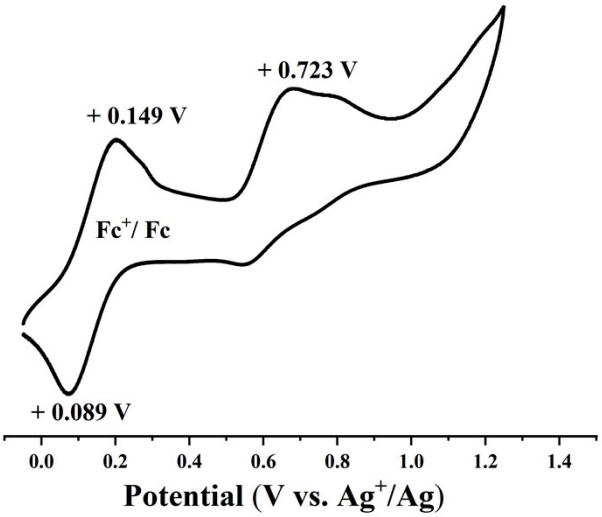

Figure S7. The cyclic voltammograms spectra of **3a** with Fc+/ Fc.

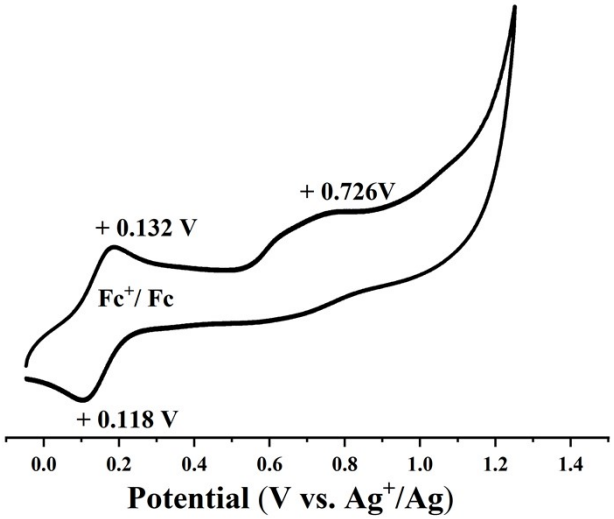

Figure S8. The cyclic voltammograms spectra of **4a** with Fc+/ Fc.

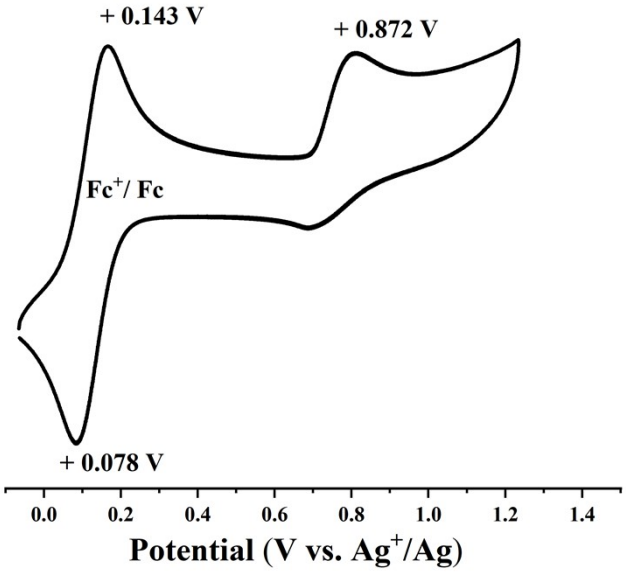

Figure S9. The cyclic voltammograms spectra of **1b** with Fc+/ Fc.

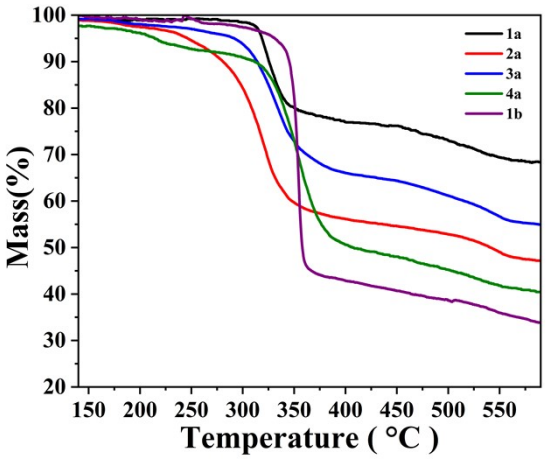

Figure S10. Thermogravimetric analyses of all the complexes.

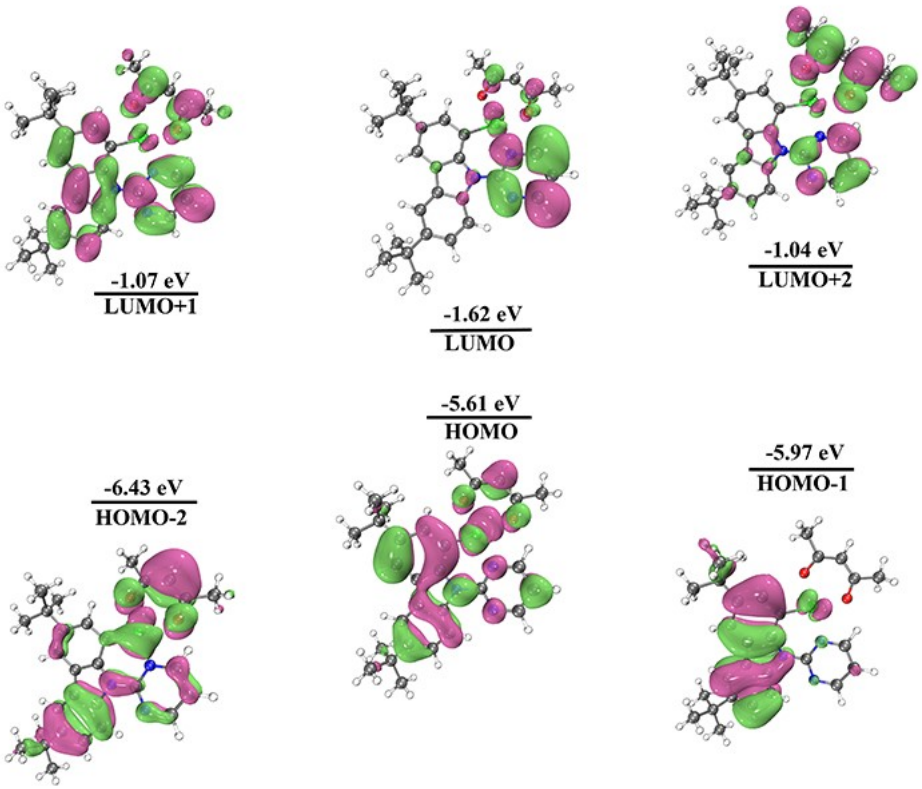

Figure S11. Molecular orbitals and energies of **1a** calculated at the lowest singlet ground state (S_0) geometry (isovalue=0.02)

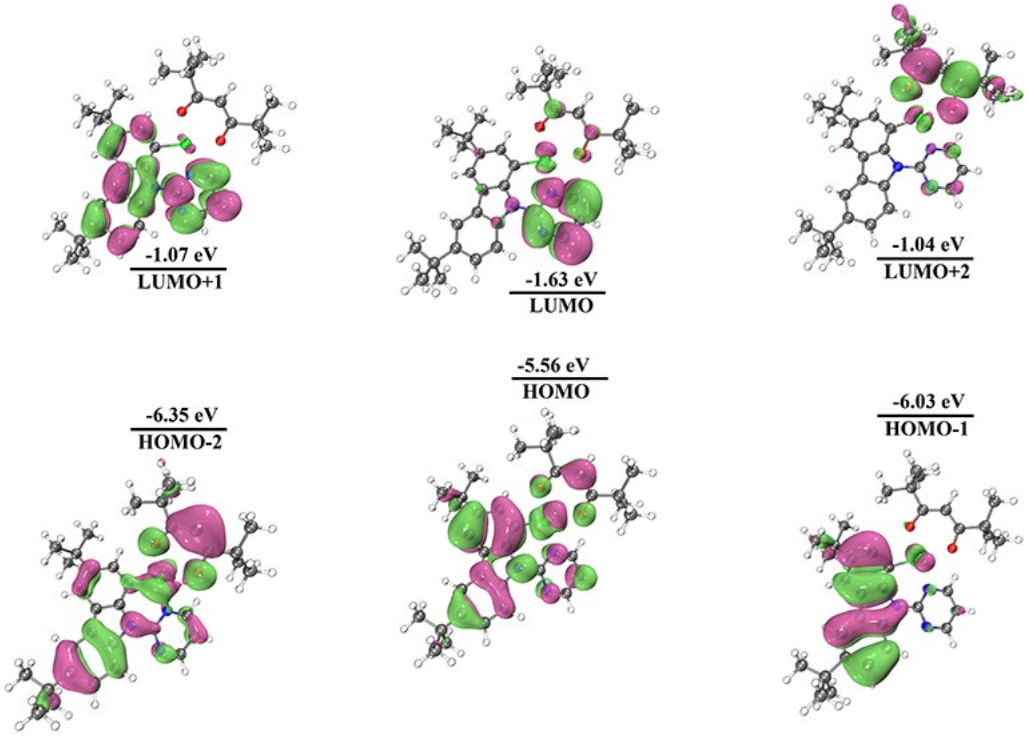

Figure S12. Molecular orbitals and energies of **2a** calculated at the lowest singlet ground state (S_0) geometry (isovalue=0.02)

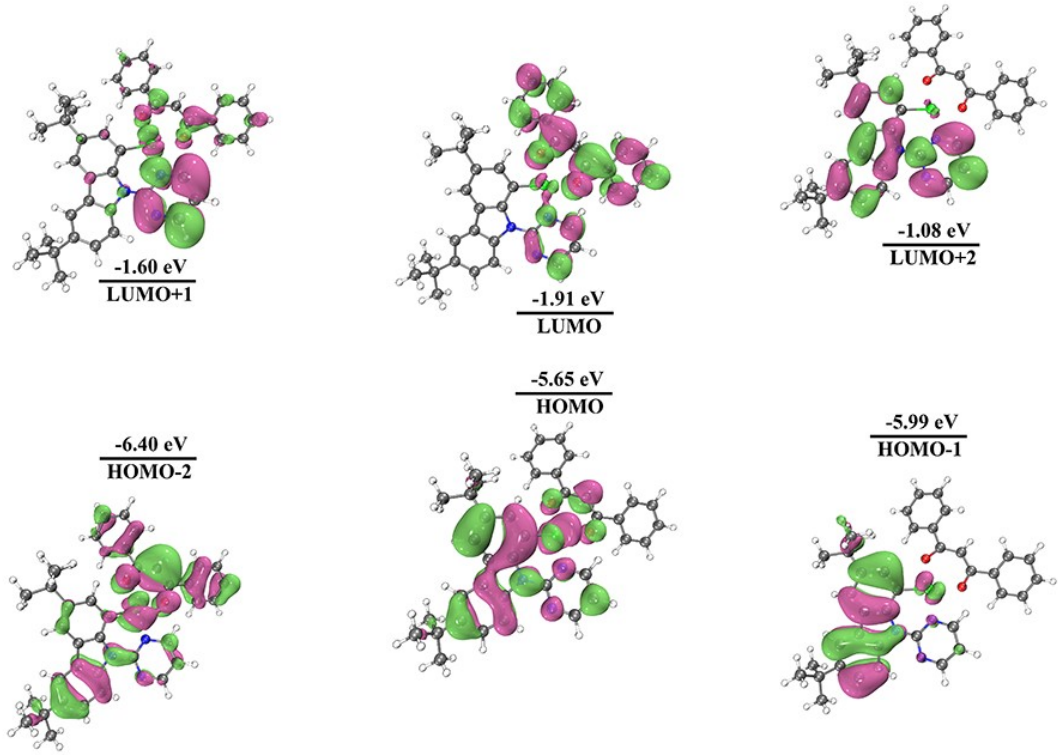

Figure S13. Molecular orbitals and energies of **3a** calculated at the lowest singlet ground state (S_0) geometry (isovalue=0.02)

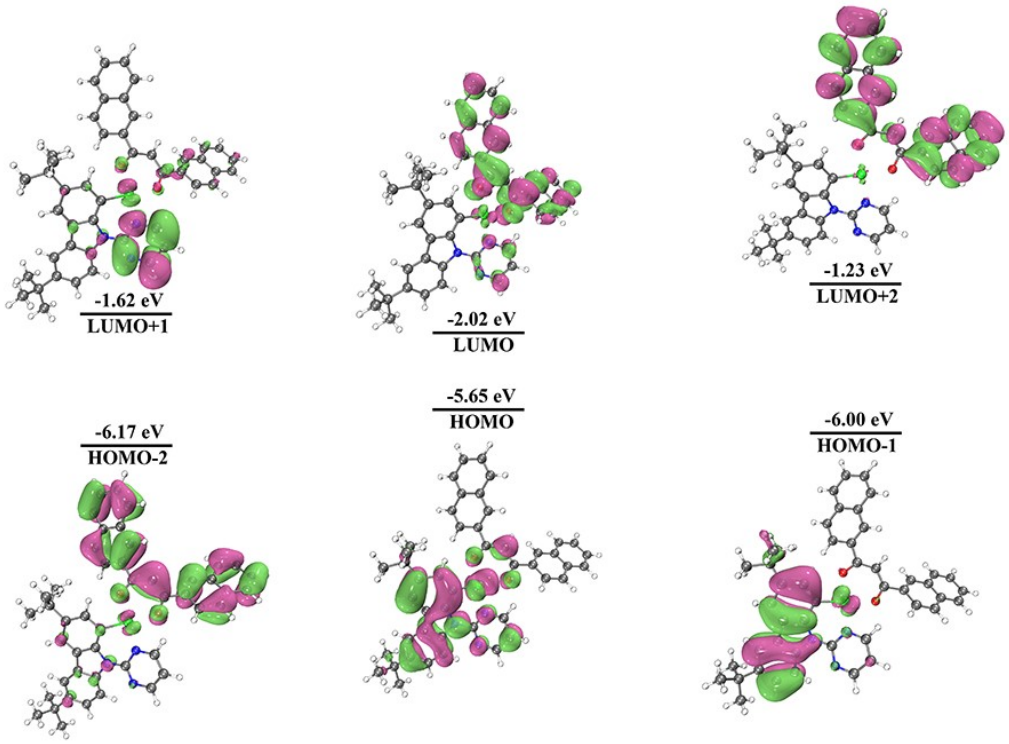

Figure S14. Molecular orbitals and energies of **4a** calculated at the lowest singlet ground state (S_0) geometry (isovalue=0.02)

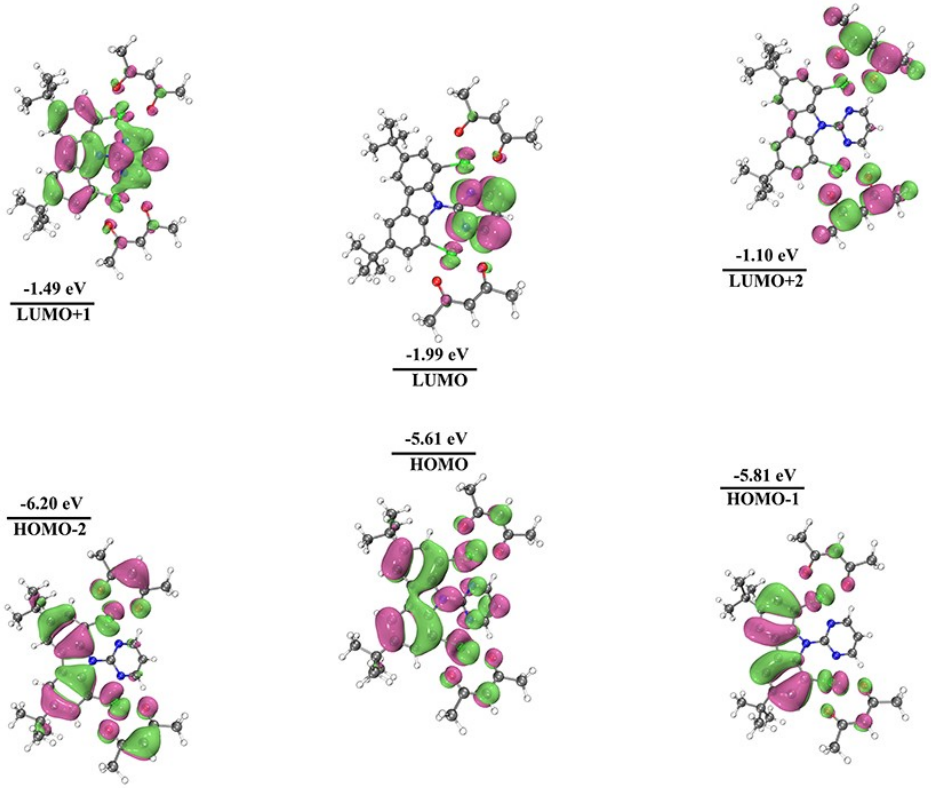

Figure S15. Molecular orbitals and energies of **1b** calculated at the lowest singlet ground state (S_0) geometry (isovalue=0.02)

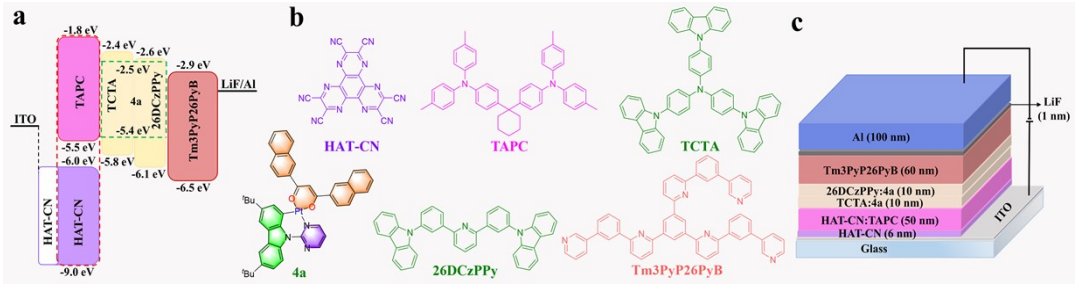

Figure S16. (a) Proposed energy-level diagram, (b) Molecule structures of each layer and (c) device structure of OLEDs based on **4a**.

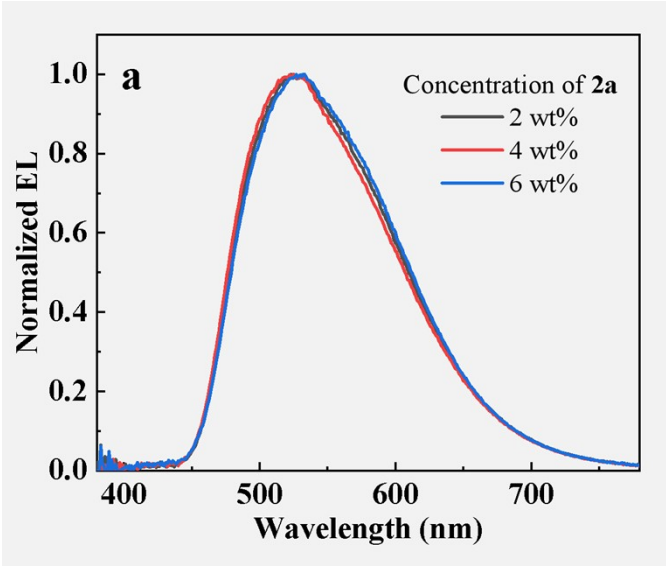

Figure S17. Normalized EL spectra of **2a** with various concentrations.

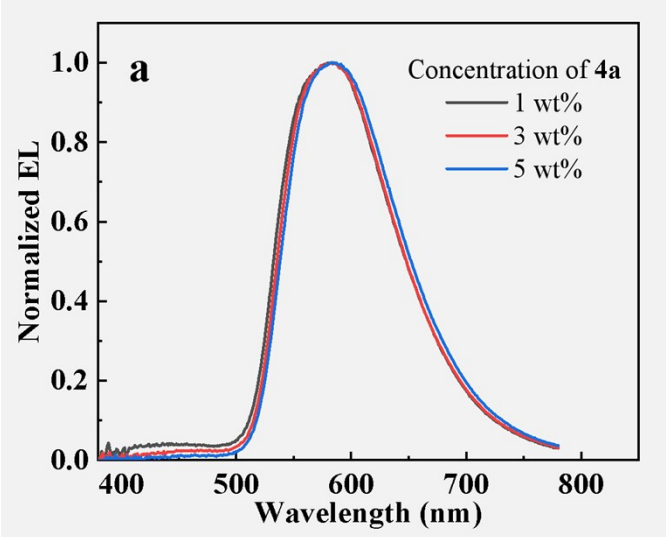

Figure S18. Normalized EL spectra of **4a** with various concentrations.

Table S1. Crystal data and structure refinement for all the complexes

	1a	1b	3a	4a-r	4a-y
CCDC number	2168891	2168892	2243237	2243261	2254329
Empirical formula	$C_{29}H_{33}N_3O_2Pt$	$C_{35}H_{41}N_3O_4Pt_2Cl_2$	$C_{39}H_{37}N_3O_2Pt$	$C_{48}H_{43}N_3O_2Pt\ Cl_2$	$C_{47}H_{41}N_3O_2Pt$
Formula weight	650.67	1028.79	774.80	959.84	874.92
Temperature/K	193.00	193.00	193.00	193.00	193.00
Crystal system	Monoclinic	Triclinic	Triclinic	Triclinic	Triclinic
Space group	$P2_1/c$	P-1	P-1	P-1	P-1
a/Å	17.3260(11)	9.2531(4)	7.1489(3)	9.3998(4)	8.8879(3)
b/Å	13.3888(8)	13.6498(7)	13.8721(6)	12.9805(4)	13.4942(4)
c/Å	11.6598(6)	14.3158(7)	17.2195(7)	17.8206(7)	17.3437(4)
α/°	90	77.502(2)	106.605(2)	78.1270(10)	70.4380(10)
β/°	107.541(2)	85.395(2)	93.658(2)	86.035(2)	81.6770(10)
γ/°	90	84.441(2)	96.398(2)	76.5340(10)	85.4040(10)
Volume/Å^3	2579.0(3)	1753.70(15)	1618.03(12)	2068.83(14)	1938.29(10)
z	4	2	2	2	2
ρ_{calc} g/cm^3	1.676	1.948	1.590	1.541	1.499
μ/mm^{-1}	5.472	8.162	4.375	3.563	3.662
F(000)	1288.0	988.0	772.0	960.0	876.0
Crystal size/mm^3	0.16 × 0.13 × 0.11	0.2 × 0.18 × 0.15	0.15 × 0.14 × 0.12	0.18 × 0.16 × 0.15	0.15 × 0.13 × 0.12
2Θ range for data collection/°	4.762 to 55.01	4.658 to 54.988	4.5 to 54.994	4.392 to 55.076	4.634 to 55.006
Index ranges	-21 ≤ h ≤ 22, -17 ≤ k ≤ 17, -15 ≤ l ≤ 14	-12 ≤ h ≤ 10, -17 ≤ k ≤ 17, -18 ≤ l ≤ 18	-9 ≤ h ≤9, -17 ≤ k ≤18, -22 ≤ l ≤ 22	-12 ≤ h ≤ 12, -16 ≤ k ≤ 16, -23 ≤ l ≤ 23	-11 ≤ h ≤ 11, -17 ≤ k ≤ 17, -19 ≤ l ≤ 22
Reflections collected	28584	34302	34200	69681	53466
Independent reflections	5901[$R_{(int)}$=0.0746, R_{sigma} =0.0564]	8021[$R_{(int)}$=0.0541, R_{sigma} = 0.0415]	7406[$R_{(int)}$=0.0479, R_{sigma}=0.0358]	9480[$R_{(int)}$=0.0480, R_{sigma}=0.0257]	8875[$R_{(int)}$=0.0606, R_{sigma}=0.0361]
Data/restraints/parameters	5901/39/355	8021/0/426	7406/0/412	9480/0/511	8875/0/484
Goodness-of-fit on F^2	1.049	1.355	1.070	1.072	1.038
Final R indexes [I>=2σ (I)]	R_1=0.0352, wR_2 = 0.0755	R_1 = 0.0613, wR_2 = 0.1412	R_1 = 0.0228, wR_2 = 0.0547	R_1 = 0.0186, wR_2 = 0.0457	R_1 = 0.0223, wR_2 = 0.0524
Final R indexes [all data]	R_1=0.0462, wR_2 = 0.0818	R_1 = 0.0621, wR_2 = 0.1421	R_1 = 0.0250, wR_2 = 0.0559	R_1 = 0.0202, wR_2 = 0.0463	R_1 = 0.0253, wR_2 = 0.0540
Largest diff. peak/ hole / e Å^{-3}	0.91/-0.89	3.41/-6.04	1.86/-0.52	0.72/-0.86	0.73/-0.42
Flack parameter	n/a	n/a	n/a	n/a	n/a

Table S2. Selected Bond Lengths and Angles for **1a**, **3a**, **4a-y**, **4a-r** and **1b**

	bond length (Å)		bond angle (deg)
1a			
Pt(1)-C(1)	1.966(5)	C(1)-Pt(1)-N(1)	91.20(18)
Pt(1)-N(1)	2.025(4)	O(1)-Pt(1)-O(2)	89.47(14)
		N(1)-Pt(1)-O(1)	178.61(14)
		C(1)-Pt(1)-O(2)	176.87(16)
3a			
Pt(1)-C(1)	1.965(3)	C(1)-Pt(1)-N(1)	91.34(10)
Pt(1)-N(1)	2.026(2)	O(1)-Pt(1)-O(2)	89.03(7)
		N(1)-Pt(1)-O(1)	179.71(7)
		C(1)-Pt(1)-O(2)	177.84(8)
4a-y			
Pt(1)-C(1)	1.961(2)	C(1)-Pt(1)-N(1)	90.96(9)
Pt(1)-N(1)	2.024(2)	O(1)-Pt(1)-O(2)	89.96(7)
		N(1)-Pt(1)-O(1)	178.65(8)
		C(1)-Pt(1)-O(2)	178.25(9)
4a-r			
Pt(1)-C(1)	1.9694(19)	C(1)-Pt(1)-N(1)	91.34(7)
Pt(1)-N(1)	2.0208(17)	O(1)-Pt(1)-O(2)	89.69(6)
		N(1)-Pt(1)-O(1)	178.63(6)
		C(1)-Pt(1)-O(2)	177.03(7)
1b			
Pt(1)-C(1)	1.969(5)	C(1)-Pt(1)-N(1)	90.98(19)
Pt(2)-C(2)	1.957(5)	C(2)-Pt(2)-N(2)	91.2(2)
Pt(1)-N(1)	2.044(4)	O(1)-Pt(1)-O(2)	88.78(16)
Pt(2)-N(2)	2.030(4)	O(3)-Pt(2)-O(4)	89.75(18)
		N(1)-Pt(1)-O(1)	177.13(17)
		N(2)-Pt(2)-O(3)	178.54(18)
		C(1)-Pt(1)-O(2)	177.33(18)
		C(2)-Pt(2)-O(4)	177.3(2)

Table S3. Frontier orbital energies, distributions, and assignments of all the complexes at the optimized S_0 geometries

	MO	Energy	MO distribution (%)				Assignment
		(eV)	d(Pt)	Cz	Py	L[a]	
1a	H-2	-6.43	15.35	27.89	6.02	50.74	d(Pt)+π(Cz+Py+L)
	H-1	-5.97	3.47	94.36	1.64	0.53	π(Cz)
	H	-5.61	21.34	58.54	9.51	10.61	d(Pt)+π(Cz+Py+L)
	L	-1.62	3.16	3.91	88.53	4.40	π*(Py)
	L+1	-1.07	2.36	34.40	44.97	18.27	π*(Cz+Py+L)
	L+2	-1.04	2.01	5.61	19.67	72.72	π*(Py+L)
2a	H-2	-6.35	12.13	24.45	5.33	50.09	d(Pt)+π(Cz+L)
	H-1	-6.03	2.94	95.09	1.55	0.42	π(Cz)
	H	-5.56	21.00	58.84	8.77	11.39	d(Pt)+π(Cz+Py+L)
	L	-1.63	3.25	3.86	89.41	3.48	π*(Py)
	L+1	-1.07	1.03	39.05	59.45	0.48	π*(Cz+Py)
	L+2	-0.96	3.34	1.84	3.32	91.50	π*(L)
3a	H-2	-6.40	10.96	18.99	4.38	65.67	d(Pt)+π(Cz+L)
	H-1	-5.99	3.46	94.29	1.53	0.72	π(Cz)
	H	-5.65	20.57	59.93	9.71	9.78	d(Pt)+π(Cz+Py+L)
	L	-1.91	1.97	0.98	11.33	85.73	π*(Py+L)
	L+1	-1.60	4.37	3.84	80.29	11.50	π*(Py+L)
	L+2	-1.08	1.03	37.51	60.90	0.55	π*(Cz+Py)
4a	H-2	-6.17	1.98	5.53	1.21	91.28	π(L)
	H-1	-6.00	3.62	93.56	1.55	1.28	π(Cz)
	H	-5.65	20.18	59.90	9.68	10.24	d(Pt)+π(Cz+Py+L)
	L	-2.02	1.87	0.60	5.58	91.95	π*(L)
	L+1	-1.62	4.10	4.01	85.45	6.45	π*(Py)
	L+2	-1.23	0.53	0.34	0.82	98.31	π*(L)
1b	H-2	-6.20	23.29	45.58	1.73	29.40	d(Pt)+π(Cz+L)
	H-1	-5.81	13.98	79.46	0.20	6.36	d(Pt)+π(Cz+L)
	H	-5.61	24.27	53.71	10.74	11.27	d(Pt)+π(Cz+Py+L)
	L	-1.99	5.32	0.93	90.97	2.78	π*(Py)
	L+1	-1.49	4.38	32.69	58.54	4.39	π*(Cz+Py)
	L+2	-1.10	3.31	4.67	1.54	90.49	π*(L)

[a] L stands for the O^O ligand.

Table S4. Excited state properties of studied complexes calculated at the optimized S_0 geometry by TDDFT

Complex	State	E/eV	λcalc./nm	*f*	Transition	Coefficient
1a	S0→S1	2.16	573.6	0.0335	HOMO→LUMO	0.70
	S0→S2	2.87	431.7	0.0133	HOMO-1→LUMO	0.70
	S0→S3	3.10	399.4	0.0008	HOMO-4→LUMO	0.60
					HOMO-3→LUMO	0.21
					HOMO-2→LUMO	0.27
2a	S0→S1	2.09	593.5	0.0318	HOMO→LUMO	0.70
	S0→S2	2.91	426.7	0.0133	HOMO-3→LUMO	0.12
					HOMO-1→LUMO	0.69
	S0→S3	3.07	403.8	0.0019	HOMO-4→LUMO	-0.24
					HOMO-3→LUMO	0.53
					HOMO-2→LUMO	-0.35
					HOMO-1→LUMO	-0.12
3a	S0→S1	2.34	530.8	0.0119	HOMO→LUMO	-0.70
	S0→S2	2.94	422.0	0.0640	HOMO-1→LUMO	0.12
					HOMO→LUMO+1	0.69
	S0→S3	3.03	408.9	0.0239	HOMO-4→LUMO	0.20
					HOMO-1→LUMO	-0.66
					HOMO→LUMO+1	0.13
4a	S0→S1	2.37	523.7	0.0188	HOMO→LUMO	0.70
	S0→S2	2.93	423.0	0.0806	HOMO→LUMO+1	0.69
	S0→S3	3.05	407.0	0.0587	HOMO-5→LUMO	0.13
					HOMO-1→LUMO	0.67
					HOMO→LUMO+1	-0.10
1b	S0→S1	2.01	616.9	0.0213	HOMO→LUMO	0.70
	S0→S2	2.46	503.4	0.0011	HOMO-2→LUMO	0.12
					HOMO-1→LUMO	-0.69
	S0→S3	2.78	446.1	0.0045	HOMO-2→LUMO	0.68
					HOMO-1→LUMO	0.13

Table S5. Excited state properties of studied complexes calculated at the optimized T_1 geometry by TDDFT.

Complex	State	E/eV	λcalc./nm	*f*	Transition	Coefficient
1a	T1	2.00	621.1	0	HOMO→LUMO (90.7%)	0.67
	T2	2.71	457.8	0	HOMO-1→LUMO (26.6%)	0.36
					HOMO-4→LUMO (21.7%)	-0.32
					HOMO-5→LUMO (11.7%)	0.24
					HOMO-2→LUMO (11.3%)	-0.24
2a	T1	1.93	642.7	0	HOMO→LUMO (92.2%)	0.68
	T2	2.71	458.3	0	HOMO-4→LUMO (36.1%)	-0.42
					HOMO-1→LUMO (19.9%)	0.31
					HOMO-5→LUMO (14.0%)	-0.26
					HOMO-2→LUMO (9.1%)	-0.21
3a	T1	2.06	603.3	0	HOMO→LUMO (55.9%)	-0.52
					HOMO-2→LUMO (37.5%)	-0.43
	T2	2.68	462.8	0	HOMO-2→LUMO (39.9%)	0.45
					HOMO→LUMO (30.9%)	-0.39
					HOMO→LUMO+1(6.3%)	0.18
					HOMO-5→LUMO (6.2%)	-0.18
4a	T1	1.70	731.3	0	HOMO-1→LUMO (52.0%)	0.51
					HOMO-1→LUMO+2(20.1%)	-0.32
					HOMO→LUMO (5.6%)	0.17
	T2	2.33	532.9	0	HOMO→LUMO (35.6%)	0.42
					HOMO-3→LUMO (24.1%)	-0.35
					HOMO-1→LUMO+2(8.3%)	0.20
					HOMO-4→LUMO (7.3%)	0.19
1b	T1	1.89	657.1	0	HOMO→LUMO (97.3%)	0.70
	T2	2.44	508.9	0	HOMO-1→LUMO (46.6%)	0.48
					HOMO-2→LUMO (21.1%)	-0.32
					HOMO-4→LUMO (9.1%)	0.21
					HOMO→LUMO+1(8.3%)	0.20

References

1 Gaussian 09, Revision E.01, M. J. Frisch, G. W. Trucks, H. B. Schlegel, G. E. Scuseria, M. A. Robb, J. R. Cheeseman, G. Scalmani, V. Barone, B. Mennucci, G. A. Petersson, H. Nakatsuji, M. Caricato, X. Li, H. P. Hratchian, A. F. Izmaylov, J. Bloino, G. Zheng, J. L. Sonnenberg, M. Hada, M. Ehara, K. Toyota, R. Fukuda, J. Hasegawa, M. Ishida, T. Nakajima, Y. Honda, O. Kitao, H. Nakai, T. Vreven, J. A. Montgomery, Jr., J. E. Peralta, F. Ogliaro, M. Bearpark, J. J. Heyd, E. Brothers, K. N. Kudin, V. N. Staroverov, T. Keith, R. Kobayashi, J. Normand, K. Raghavachari, A. Rendell, J. C. Burant, S. S. Iyengar, J. Tomasi, M. Cossi, N. Rega, J. M. Millam, M. Klene, J. E. Knox, J. B. Cross, V. Bakken, C. Adamo, J. Jaramillo, R. Gomperts, R. E. Stratmann, O. Yazyev, A. J. Austin, R. Cammi, C. Pomelli, J. W. Ochterski, R. L. Martin, K.

Morokuma, V. G. Zakrzewski, G. A. Voth, P. Salvador, J. J. Dannenberg, S. Dapprich, A. D. Daniels, O. Farkas, J. B. Foresman, J. V. Ortiz, J. Cioslowski, and D. J. Fox, Gaussian, Inc., Wallingford CT, 2013.

2 T. Lu and F. Chen, Multiwfn: a multifunctional wavefunction analyzer, *J. Comput. Chem.*, 2012, **33**, 580-592.

3 W. Humphrey, A. Dalke and K. Schulten, VMD: visual molecular dynamics, *J. Mol. Graph.*, 1996, **14**, 33-38, 27-38.

4 X. Zhao, Y. She, K. Fang and G. Li, CuCl-Catalyzed Ullmann-Type C-N Cross-Coupling Reaction of Carbazoles and 2-Bromopyridine Derivatives, *J. Org. Chem.*, 2017, **82**, 1024-1033.

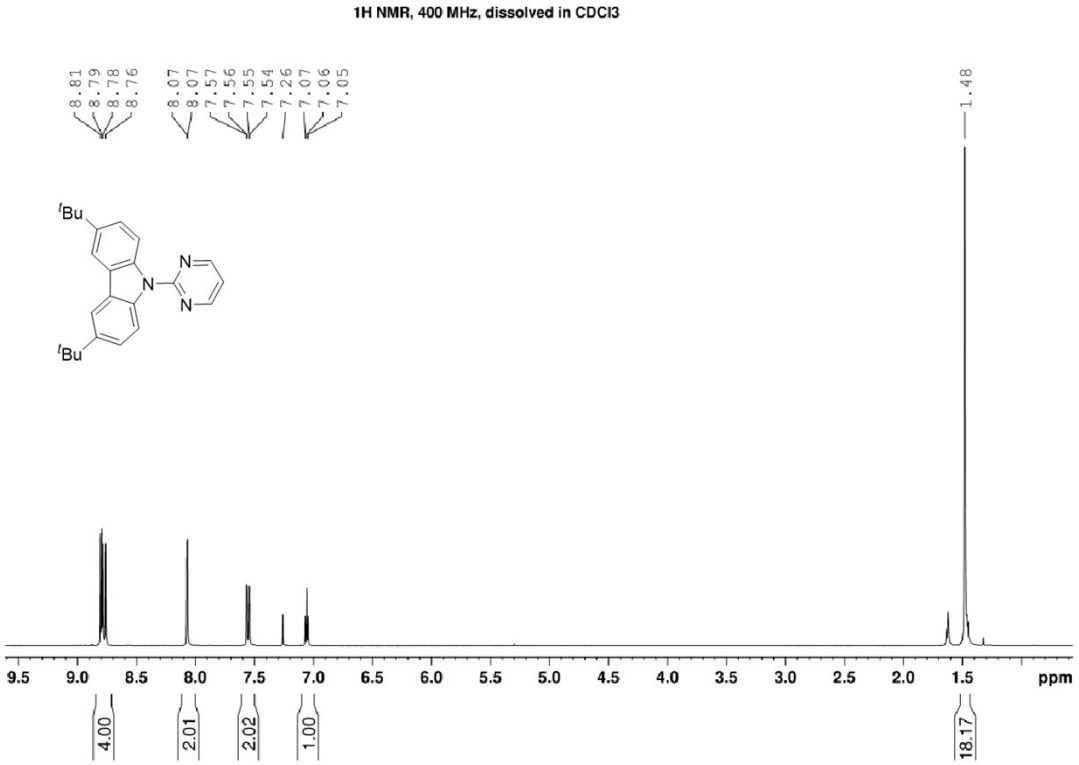

Figure S19. ^{1}H NMR spectrum of **TBPCH$_2$** ($CDCl_3$)

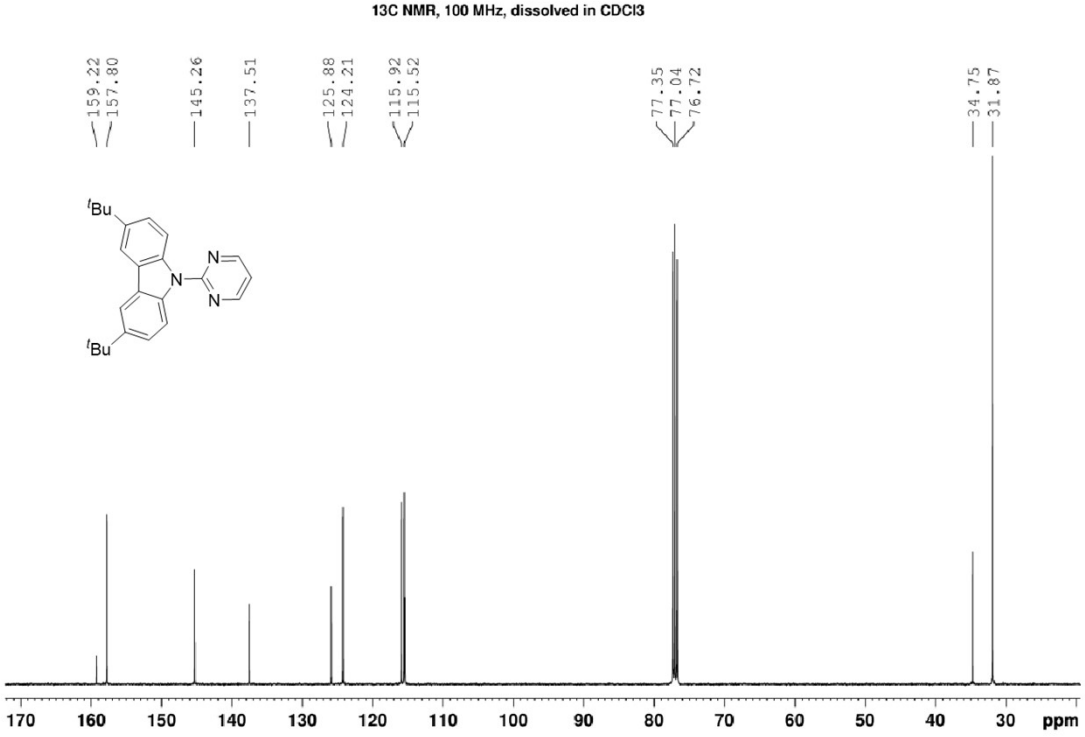

Figure S20. ^{13}C NMR spectrum of **TBPCH$_2$** ($CDCl_3$)

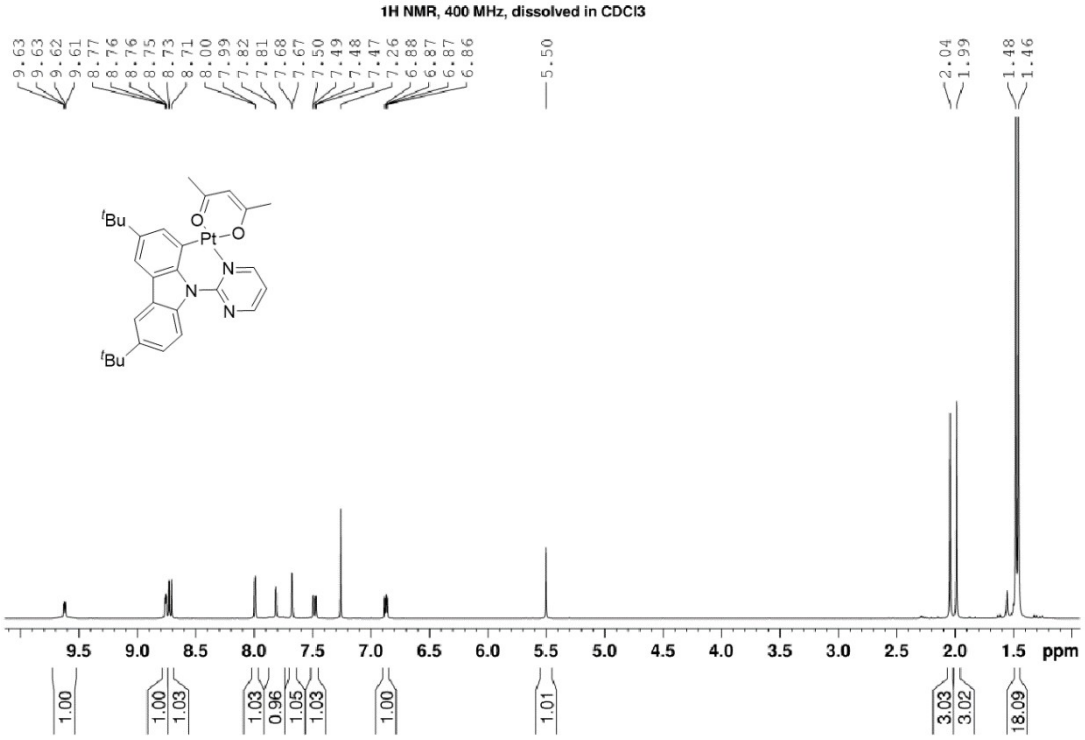

Figure S21. ^{1}H NMR spectrum of **1a** ($CDCl_3$)

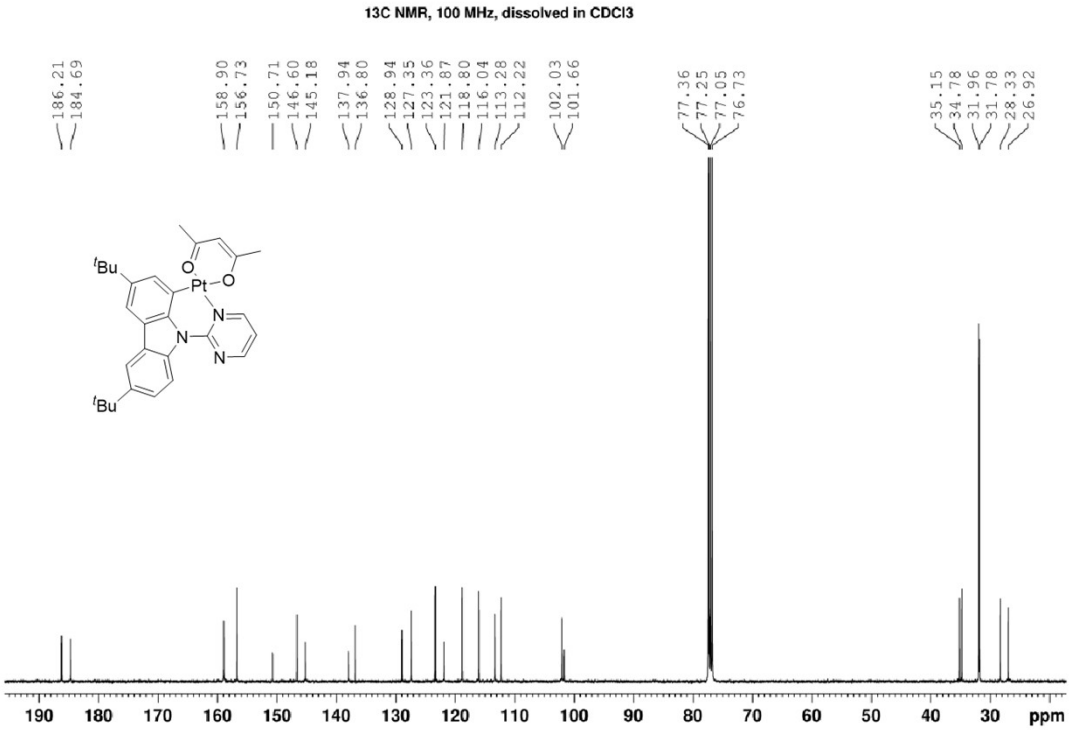

Figure S22. ^{13}C NMR spectrum of **1a** ($CDCl_3$)

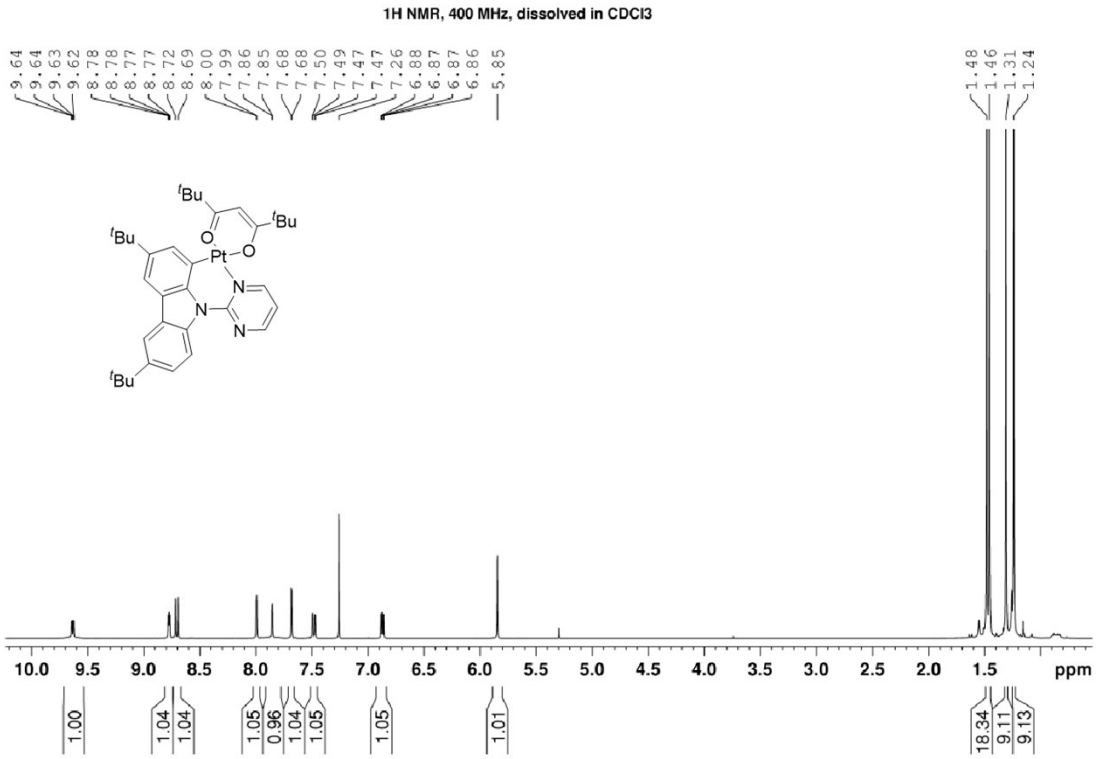

Figure S23. ^{1}H NMR spectrum of **2a** ($CDCl_3$)

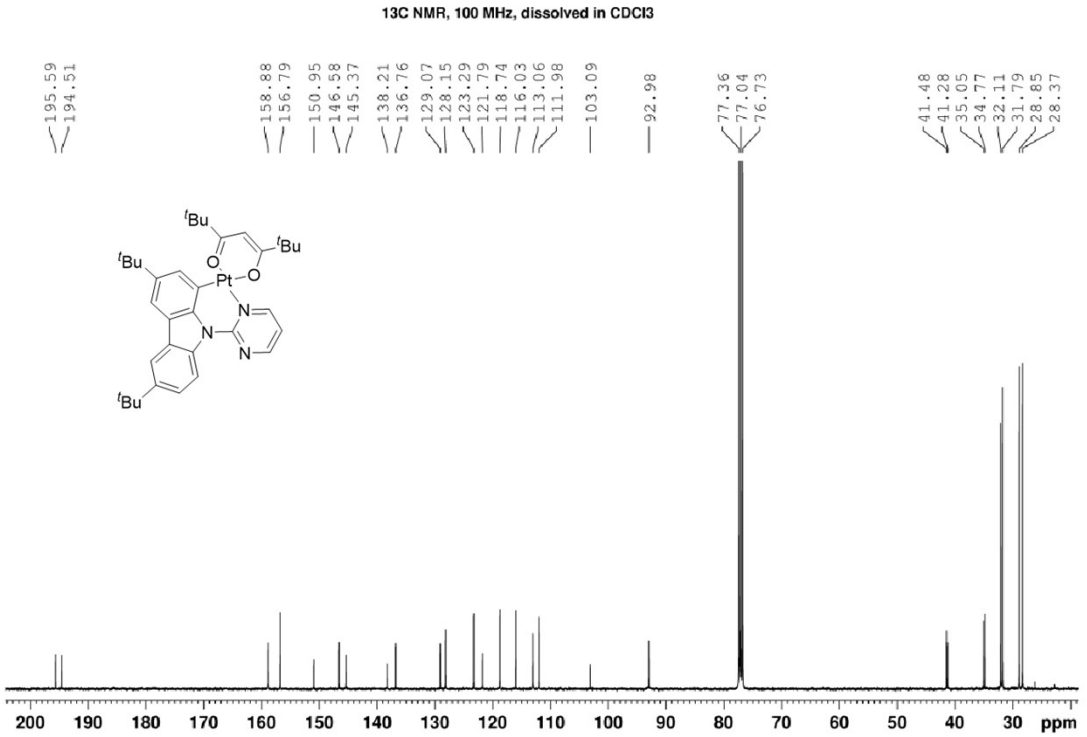

Figure S24. ^{13}C NMR spectrum of **2a** ($CDCl_3$)

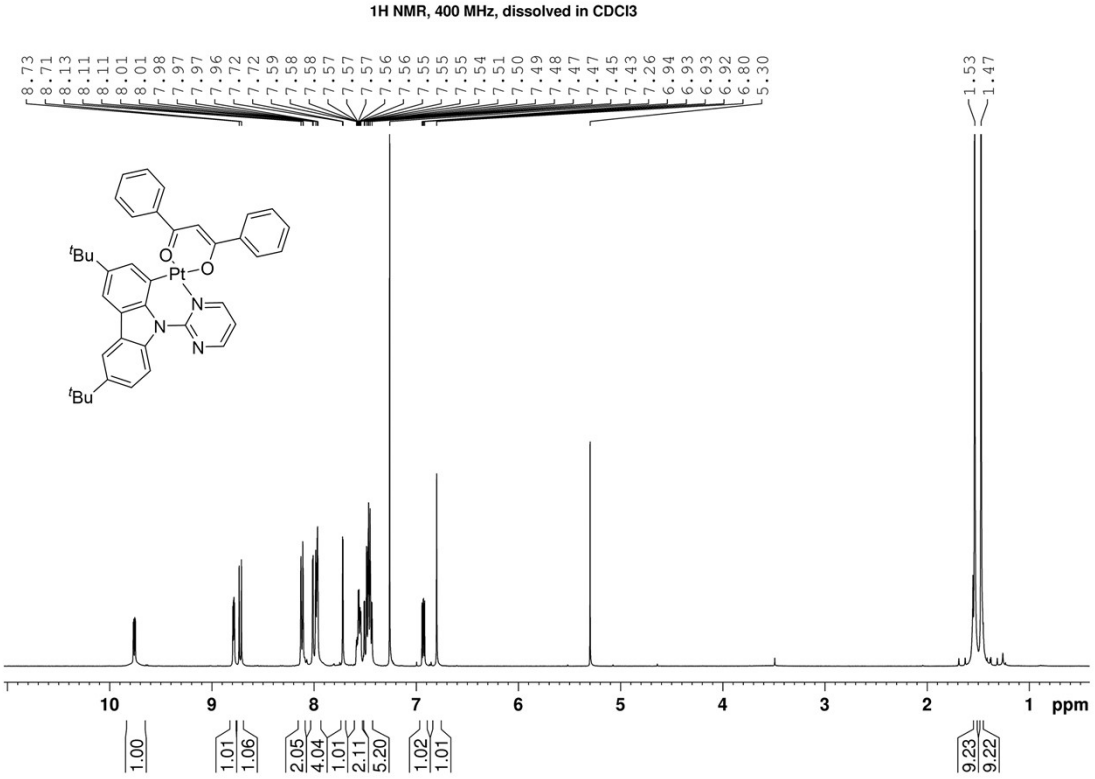

Figure S25. ^{1}H NMR spectrum of **3a** ($CDCl_3$)

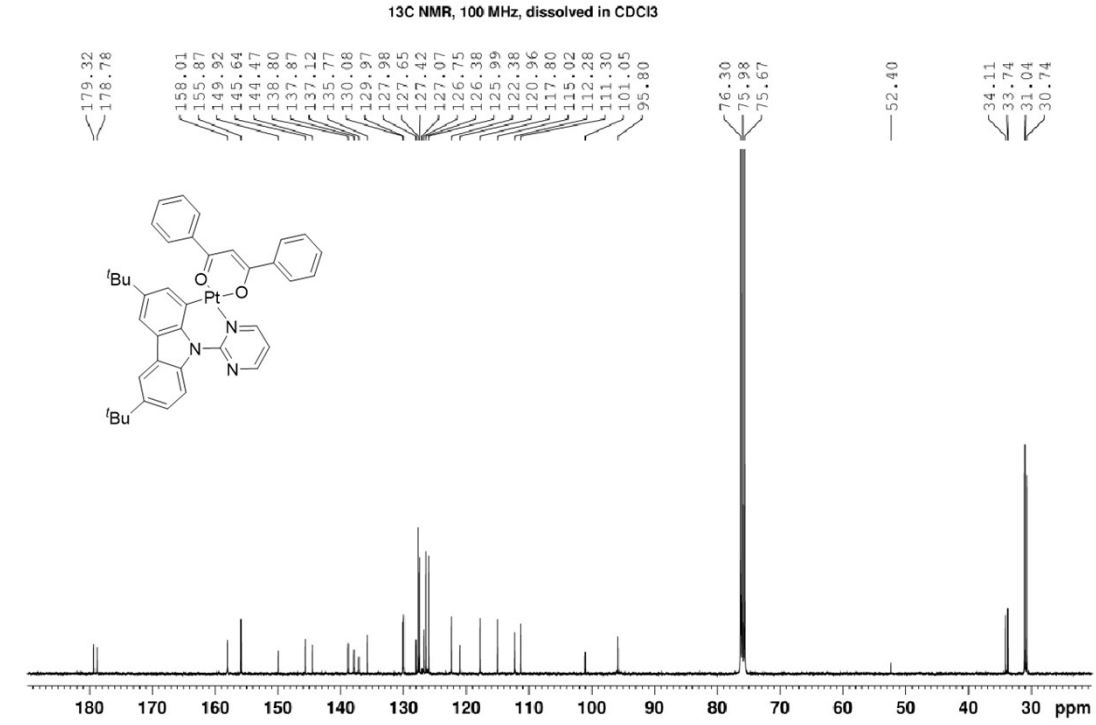

Figure S26. ^{13}C NMR spectrum of **3a** ($CDCl_3$)

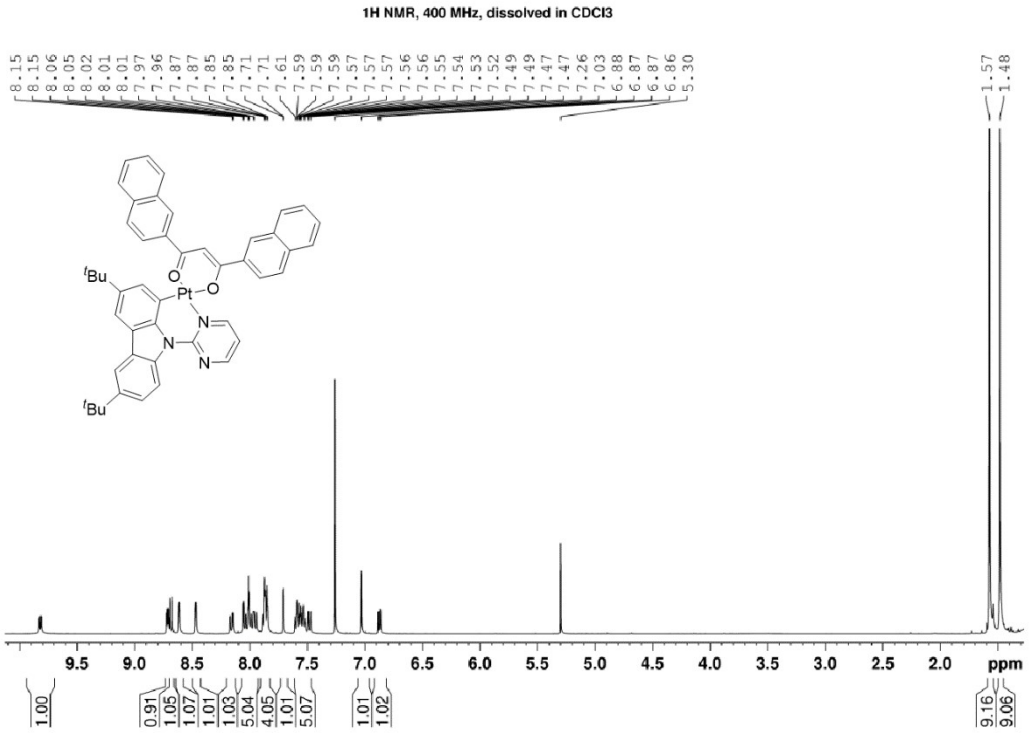

Figure S27. ^{1}H NMR spectrum of **4a** ($CDCl_3$)

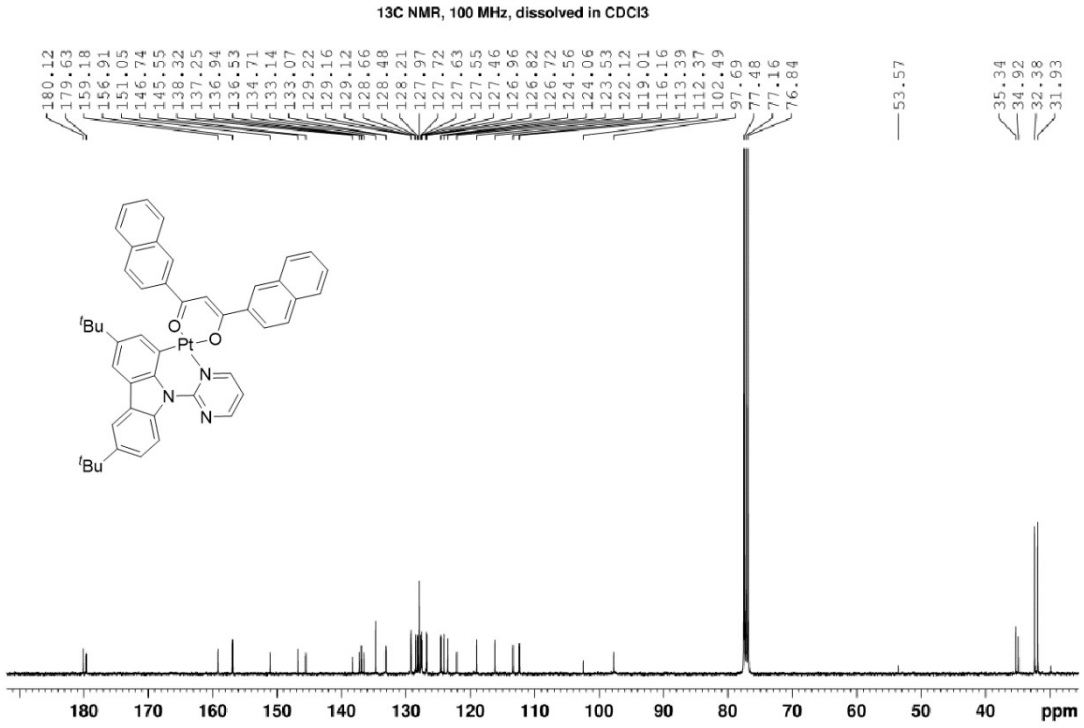

Figure S28. ^{13}C NMR spectrum of **4a** ($CDCl_3$)

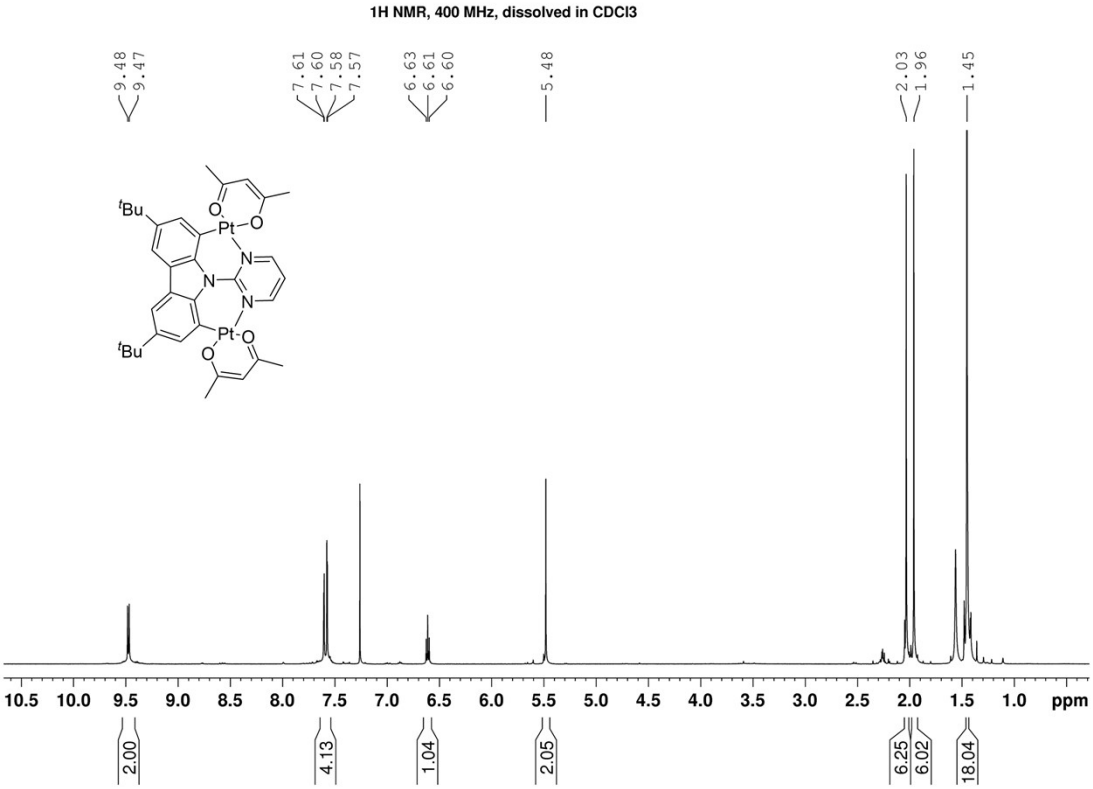

Figure S29. ^{1}H NMR spectrum of **1b** ($CDCl_3$).

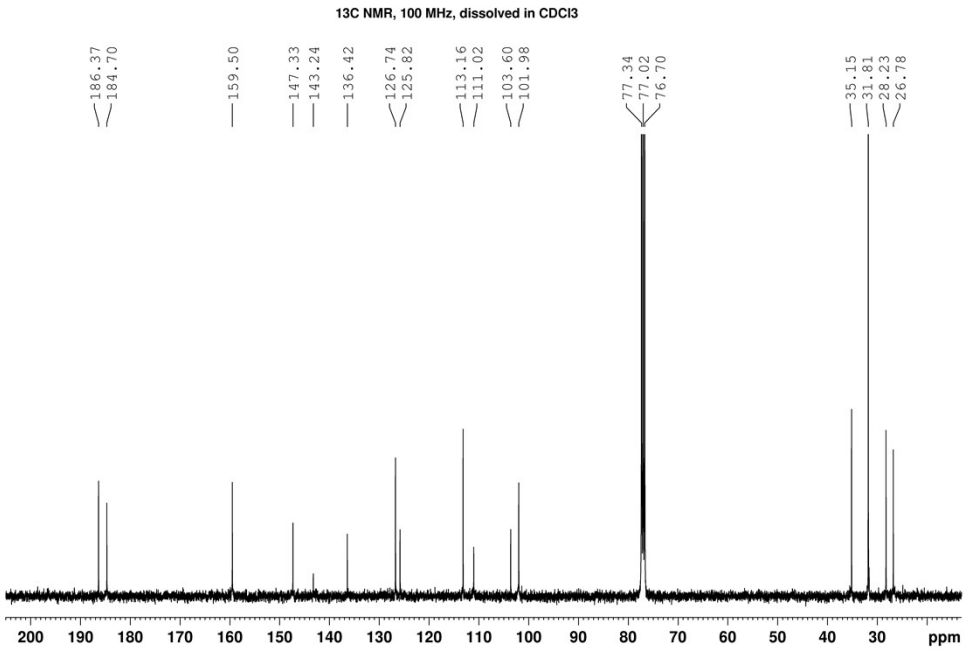

Figure S30. ^{13}C NMR spectrum of **1b** ($CDCl_3$)

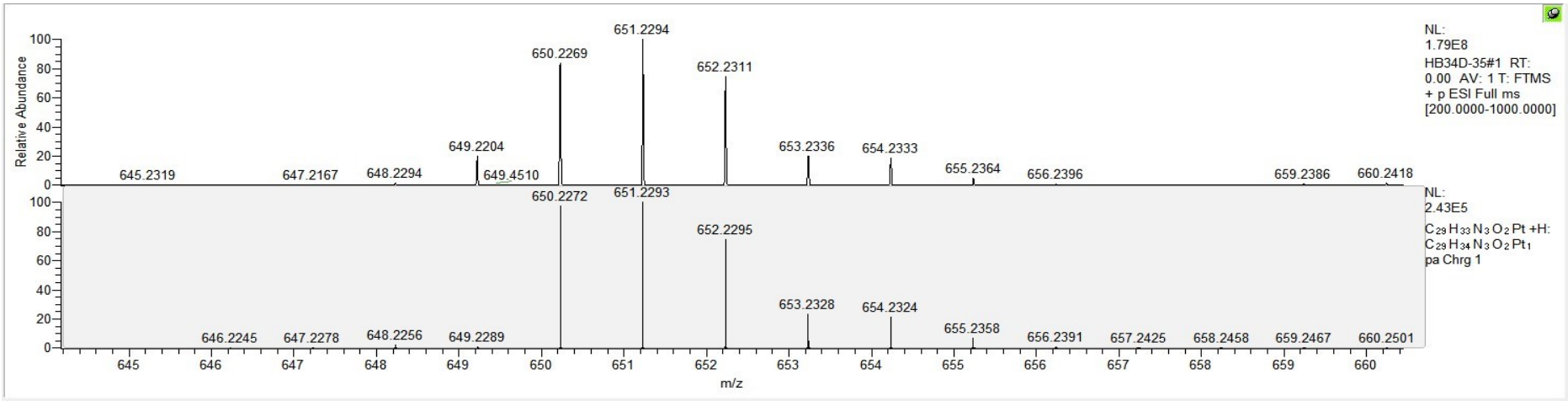

Figure S31. HRMS spectra for **1a** $[M + H]^+$.

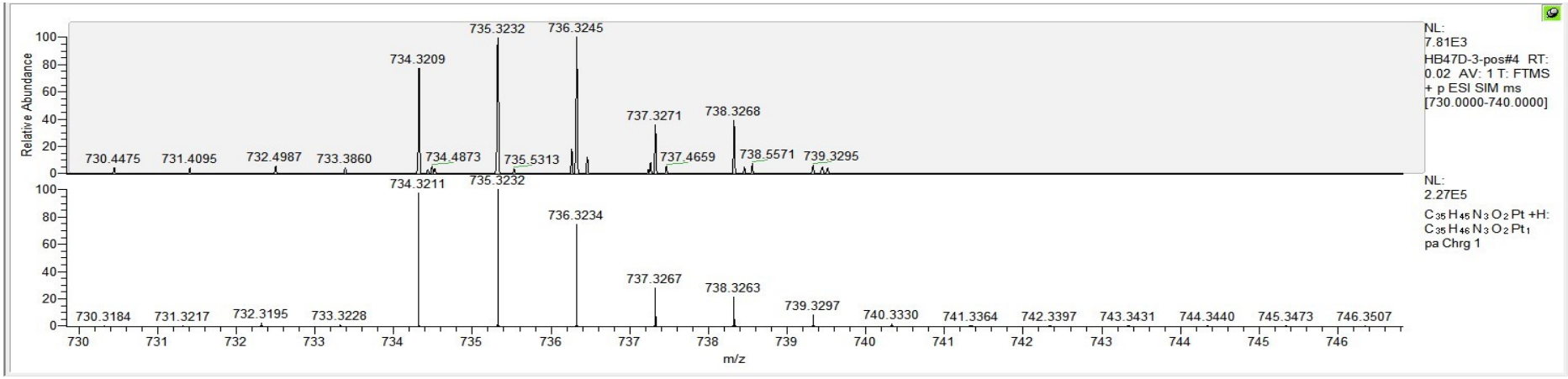

Figure S32. HRMS spectra for **2a** $[M + H]^+$.

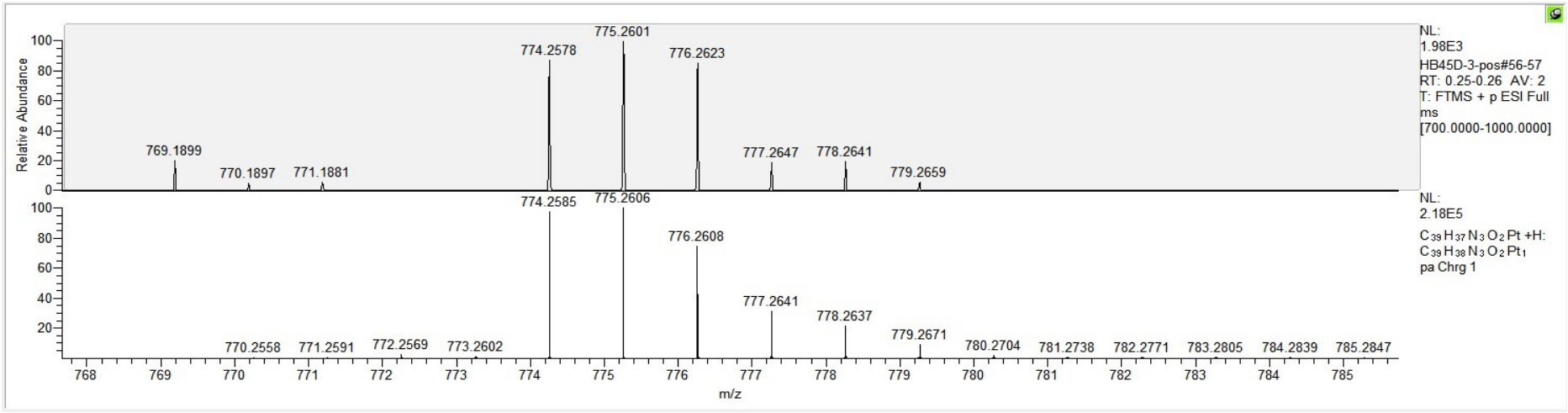

Figure S33. HRMS spectra for **3a** $[M + H]^+$.

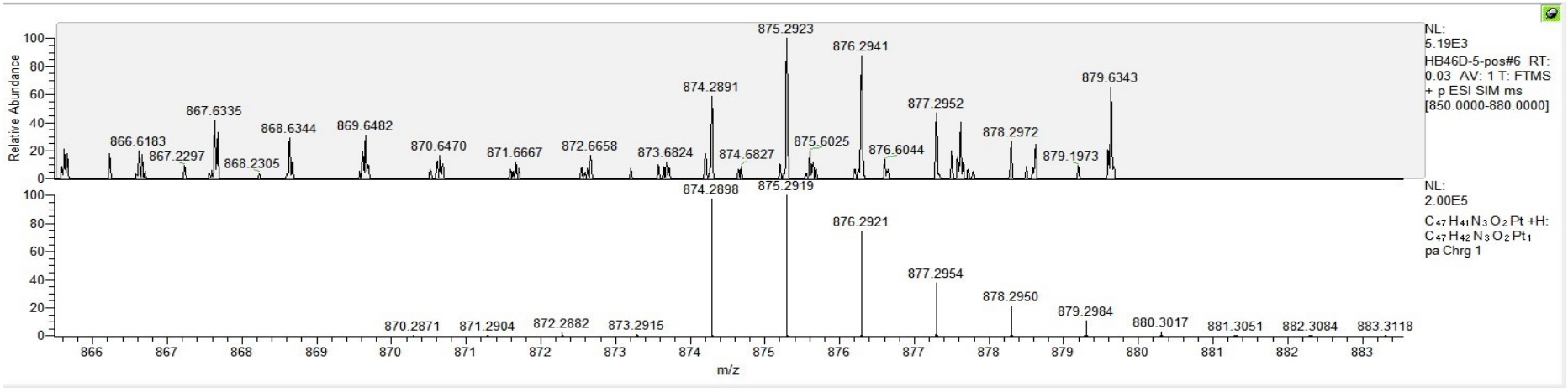

Figure S34. HRMS spectra for **4a** $[M + H]^+$.

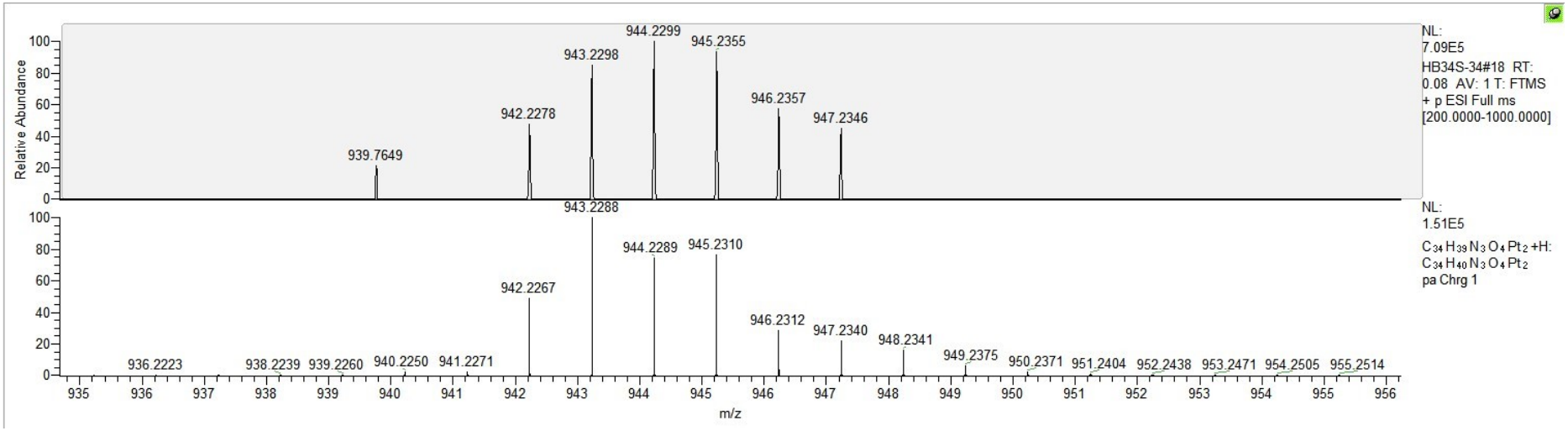

Figure S35. HRMS spectra for **1b** $[M + H]^+$.